

Designing Feedback Controllers for Human-Prosthetic Systems Using H_∞ Model Matching

Julia Costacurta¹, Luke Osborn¹, Nitish Thakor¹ and Sridevi Sarma^{1,2}

Abstract—Prosthetic hands are important tools for improving the lives of upper limb amputees, yet most devices lack the ability to provide a sense of touch back to the user. Recent improvements have been made in electromyography (EMG) prosthesis control that use more biologically relevant tactile sensors and that provide sensory feedback to amputees through nerve stimulation. However, sensory feedback has been designed heuristically, which can lead to either unnatural sensations or to excessive feedback that bothers the user. In this study, we apply optimal control techniques to synthesize sensory feedback to the user, and to synthesize the conversion from EMG to an actuation command to the prosthesis. Specifically, we construct a feedback control system architecture and solve the H_∞ model matching problem to make the closed-loop user-prosthetic system to behave like a pre-specified ideal system in response to elemental inputs (e.g. impulse, step, etc). We design feedback controllers assuming that human and prosthetic components behave in a linear fashion as a proof-of-concept, and the closed-loop system is able to match ideal systems that are slow, fast and that have both slow and fast dynamics (like healthy humans).

I. INTRODUCTION

Prosthetic hands are important tools for improving the lives of upper limb amputees; however, most of these devices lack the ability to feedback a sense of touch to the user. Prosthesis users typically rely on visual feedback to accomplish tasks with their devices. Avoiding grasping objects with too much force or allowing objects to slip through the fingers of the prosthesis are often concerns for users. A more natural human-prosthesis interface would allow the human to actuate the prosthesis, and the prosthesis to in turn allow the human to feel what the prosthetic hand touches. This is critical for picking up, holding, or manipulating objects with their prosthesis. In healthy hands, numerous mechanoreceptors within the skin allow for our sense of touch and make up the closed-loop tactile feedback system that provides us with valuable information regarding our environment [1], [2].

Recent improvements have been made in electromyography (EMG) prosthesis control, specifically in pattern recognition strategies [3], [4], more biologically relevant tactile sensors [5], [6], and even sensory feedback to amputees through nerve stimulation [7], [8]. Although the technology used to build prosthetic limbs continues to advance at a rapid pace, there is still much to be done in order to make the interface between a prosthesis and a user as natural as possible. Researchers have proposed more biologically

relevant stimulation approaches for sensory feedback [9], [10] (Fig. 1), but one challenge is deciding when and how to provide sensory feedback to a user. More specifically, how that sensory perception is interpreted and ultimately incorporated into the prosthesis control model of the user is unknown. In healthy humans, touch information is used to help refine motor movements to complete complex tasks through continuous closed-loop feedback, but for upper limb prosthesis users this type of completely natural and seemingly automated behavior where motor commands are linked to the input from the tactile signal, such as a reflex, is not present. A common example of this behavior in an able-bodied individual would be recoiling from a hot surface or making subtle changes to grip force while handling an object to prevent it from falling. It is important that upper limb prostheses mimic this behavior to give a natural sense of control for a user.

In the case of sensory feedback to a user, there is often a processing delay as the user attempts to interpret the information. This is especially true for types of feedback that provide sensory substitution to the user [11], [12]. Although more natural sensory feedback is possible through direct nerve electrical stimulation [7], [9], how this information is used for a feedback control model is still unknown. The added cognitive load of unnatural sensory feedback processing can cause the loss of valuable seconds before a response is made compared to the more natural reflex actions found in able-bodied individuals. Excessive sensory feedback can also prove bothersome to a prosthesis user when too many feedback mechanisms are used simultaneously [13]. Thus, some midpoint between prosthesis and user control must be reached in order to create the ideal prosthesis-user system. Control theory offers an interesting tool to meet this challenge.

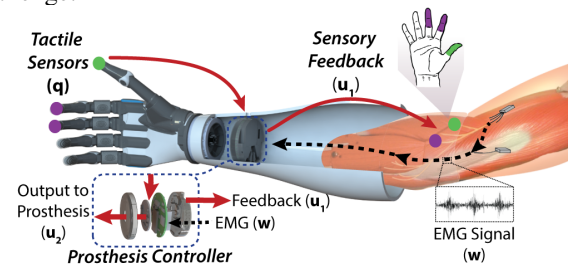


Fig. 1. Overview of a closed-loop system for a prosthetic limb with variable labels. Muscle activity (EMG) from an amputee is used by the prosthesis controller to send movement commands to the prosthetic hand. Tactile sensors on the prosthesis measure force during object grasping and are used as feedback to the controller. Touch information can be conveyed back to the amputee user in the form of sensory feedback from peripheral nerve stimulation.

*This work was not supported by any organization

¹Biomedical Engineering Department, Johns Hopkins University, Baltimore, MD, USA jcostacl@jhu.edu

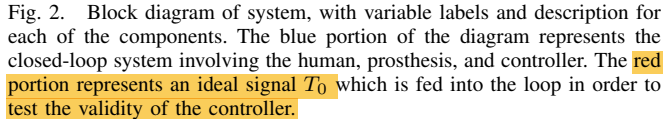
²Institute for Computational Medicine, Johns Hopkins University, Baltimore, MD, USA ssarma2@jhu.edu

Various controllers have already been implemented to translate user EMG data into an actuating input to a prosthetic arm forming a brain-machine interface, as described in [16]. However, designing a controller that both processes EMG data to actuate the prosthesis *and* also provides sensory feedback to the user based on prosthesis output still requires investigation. Such a controller would allow for even more natural control of a prosthesis by a user by taking into account how sensory feedback influences the forward control model implemented by the user, thus allowing the user to "feel" the prosthesis like his/her own natural arm.

II. METHODS

A. Closed-loop model of user-prosthetic system

We can represent this closed-loop system, with the **human in the loop, in a block diagram form** as shown in the top blue portion of Fig. 2. The bottom red portion represents an ideal system T_0 that we wish the closed-loop system to mimic (e.g. a healthy human). In the top portion of Fig. 2, $r(t)$ represents a reference trajectory that the subject wishes the prosthesis to follow (likely generated in the parietal region of the brain). This in turn will generate a response from the user-prosthesis system, $q(t)$, which is fed back into the first controller, K_1 , which represents the processor that converts the tactile signals into a stimulation signal given by u_1 . This



We wish this closed-loop user-prosthetic system to behave like a pre-specified ideal system T_0 shown in red. That is, our goal is to design K_1 and K_2 such that the infinity norm of the error system, $E(s) = H_{CL}(s) - T_0(s)$, is minimized. Note that H_{CL} is the closed loop system from z to q and a function of K_1, K_2, H , and P . H and P can be estimated based data from experimental observations. More specifically, we solve the following model matching problem for our user-prosthetic system:

$$\begin{aligned} & \min_{K_1, K_2} \|H_{CL}(K_1, K_2) - T_0\|_{H_\infty} \quad (1) \\ & \text{s.t. } H_{CL} \text{ is stable.} \end{aligned}$$

$$\|H\|_{\infty} = \sup_{\omega} \sigma(H(j\omega)) \quad (2)$$

The H_∞ norm of a multi-input multi-output system essentially is the upper bound on the gain that the system can apply to an input with finite energy. In our case, the H_∞ controllers are the K_1 and K_2 that minimize the error between the actual and ideal system, as represented in Equation (1). This model matching problem is solved via the Youla parametrization [19], and is implemented in MATLAB's control toolbox. To use the H_∞ controller design capabilities of MATLAB, we first rearranged the block diagram above in the linear fractional transformation (LFT) form as shown in Fig. 3. The LFT is expanded in Fig. 4, and is a convenient and powerful formulation in control system analysis and controller synthesis [17]. In

the LFT, the controller components are separated from the remainder of the system, where G is the system as viewed from all controllers. In our example, G has three inputs: r and $\mathbf{u} = [u_1 \ u_2]^T$; and three outputs: e and $\mathbf{y} = [q \ w]^T$. The multi-input multi-output controller, K , has two inputs $\mathbf{y} = [q \ w]^T$ and two outputs $\mathbf{u} = [u_1 \ u_2]^T$. Recall that as shown in Fig. 2, $z = r - u_1$ and w is the EMG signal from the amputee's residual limb.

B. State-space model for G

We implement MATLAB's function `hinfstruct` to help solve our model matching problem. To do so, we first derive a state-space representation of $G = ss(A, B, C, D)$ given state-space representations of H , P , and T_0 . Using the interconnection shown in Fig. 4, it is possible to derive the state-space model of G , from the state-space models of T_0 , P , and H as follows. Let

$$T_0 : \begin{aligned} \dot{x}_{T_0} &= A_{T_0}x_{T_0} + B_{T_0}r \\ v &= C_{T_0}x_{T_0} + D_0r \end{aligned}$$

$$P : \begin{aligned} \dot{x}_P &= A_Px_P + B_Pu_2 \\ q &= C_Px_P + D_Pu_2 \end{aligned}$$

$$H : \begin{aligned} \dot{x}_H &= A_Hx_H + B_Hz \\ w &= C_Hx_H + D_Hz \end{aligned}$$

Then from Fig. 4 the following relations are true:

$$e = v - q \quad z = r - u_1$$

So, we can rewrite

$$\begin{aligned} e &= v - q = C_{T_0}x_{T_0} + D_0r - (C_Px_P + D_Pu_2) \\ w &= C_Hx_H + D_Hz = C_Hx_H + D_H(r - u_1) \end{aligned}$$

using the definitions from above. Then, we need to arrange this to give:

$$G : \begin{aligned} \dot{x}_G &= [\dot{x}_{T_0} \ \dot{x}_P \ \dot{x}_H]^T = A_Gx_G + B_G[r \ u_1 \ u_2]^T \\ [e \ q \ w]^T &= C_Gx_G + D_G[r \ u_1 \ u_2]^T \end{aligned}$$

where x_G is the closed-loop state vector, $[e \ q \ w]^T$ is the output vector, and $[r \ u_1 \ u_2]^T$ is the input vector. Looking at the above equations, we can write:

$$A_G = \begin{bmatrix} A_{T_0} & 0 & 0 \\ 0 & A_P & 0 \\ 0 & 0 & A_H \end{bmatrix}, B_G = \begin{bmatrix} B_{T_0} & 0 & 0 \\ 0 & 0 & B_P \\ B_H & -B_H & 0 \end{bmatrix}$$

$$C_G = \begin{bmatrix} C_{T_0} & -C_P & 0 \\ 0 & C_P & 0 \\ 0 & 0 & C_H \end{bmatrix}, D_G = \begin{bmatrix} D_{T_0} & 0 & -D_P \\ 0 & 0 & D_P \\ D_H & -D_H & 0 \end{bmatrix}$$

which gives us the state space model for G . It is important to note that K is a diagonal controller with K_1 and K_2 along the diagonal. This imposes structure on our model matching problem.

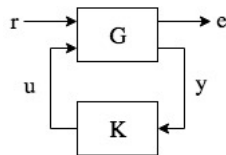


Fig. 3. Configuration of block diagram for use of H-infinity synthesis commands in MATLAB. The block K contains controllers K_1 and K_2 in a diagonal structure, and the block G contains information from P , H , and a user-specified T_0 . The input to this system is the desired reference signal, and the output is the error between the output of T_0 and the output of CL .

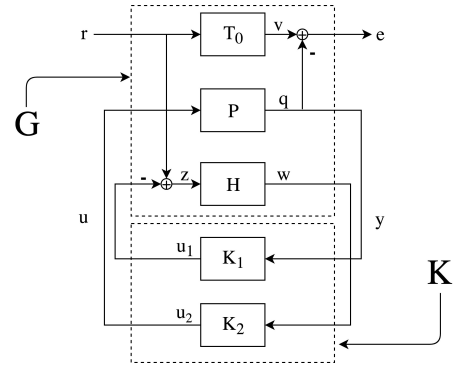


Fig. 4. Expanded Block Diagram. Here, the block diagram from Fig. 2 has been rearranged to fit the form specified in Fig. 3. This block diagram is used to determine the state space model of the G , thus preparing to use H-infinity synthesis.

III. RESULTS AND DISCUSSION

The MATLAB command `hinfstruct` can be used to minimize the H_∞ -norm of a system by tuning the two controllers with variable parameters along the diagonal of K . To demonstrate performance of our framework on LTI systems, we specified transfer functions for H , P , and T_0 to tune two second-order K_1 and K_2 . The two optimal controllers, can then be implemented to create H_{CL} as represented in Fig. 2. Note that the closed-loop transfer function from r to q is $H_{CL}(s) = \frac{H * K_2 * P}{1 + K_1 * H * K_2 * P}$.

For this proof-of-concept study, we approximated the human block H with a first-order transfer function with a response time of 70-100 ms. This response time specification and assumption for H represents a reflex pathway for slip prevention during grasping [18]. The prosthesis block P is also represented with a first-order transfer function, based on previous examples [20], with a slower response time than that of the human transfer function. In particular, we let

$$P = \frac{1}{s+1}, \quad H = \frac{50}{s+50}.$$

To test our code, we used three different T_0 transfer functions that are first and second order systems:

$$T_0^{fast} = \frac{100}{s+100} \quad (3)$$

$$T_0^{slow} = \frac{10}{s+10} \quad (4)$$

$$T_0^{fast-slow} = \frac{1000}{(s+10)(s+100)} \quad (5)$$

Recall, the first order systems do not oscillate, while second order systems may oscillate. These three examples were chosen because Equations (3) and (4) have fast and slow response times, respectively; and Equation (5) is a second order system that exhibits both slow and fast dynamics. Here, having a fast response time means that the system will react quickly to an input, and a slower response time means the system takes more time to react (as in slow and fast adapting tactile sensors in our fingers). Equations (3) and (5) produce the optimal closed-loop transfer functions, H_{CL}^* with outputs shown in Fig. 5. The signals u_1^* and u_2^* , corresponding to the electrical stimulation signal for the user and the actuation

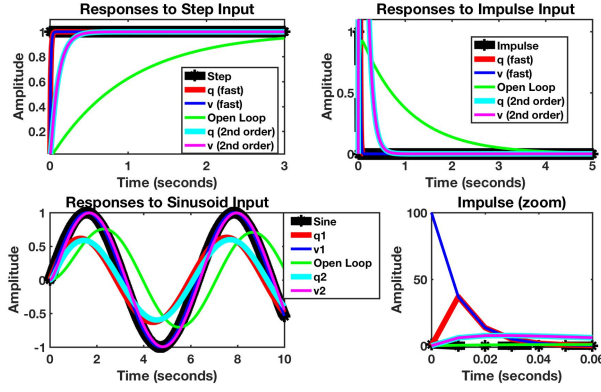


Fig. 5. Responses to step, impulse, and sinusoidal inputs for H_{CL} and T_0 . The system H_{CL} is consistent with the H_{CL} described in Fig. 2, with q as the response of H_{CL} and v as the response of T_0 .

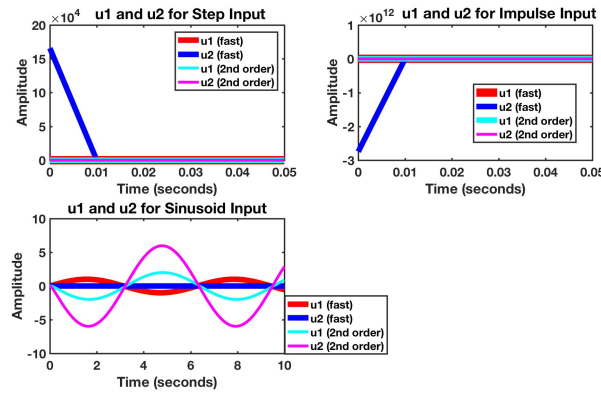


Fig. 6. The output from K_1 , u_1 , and actuation signal u_2 required to produce the outputs given in Fig. 5.

signal, respectively, are given in Fig. 6. These optimal control inputs were calculated by finding the transfer functions from r to u_1 and r to u_2 from Fig. 2.

In order to test the accuracy of our method for various types of T_0 , we computed the respective error norms for each closed-loop error system as shown in Fig. 7. Our results show that our H_∞ framework is more accurate at matching slower T_0 functions than faster ones, and is able to match second-order transfer functions more accurately than first-order transfer functions. This is intuitive as a slow system is less demanding than a fast system and a second order system allows for more flexibility in control design. The 2-norms of the controller-generated signals u_1 and u_2 for step, impulse, and sinusoid inputs are shown in Fig. 8.

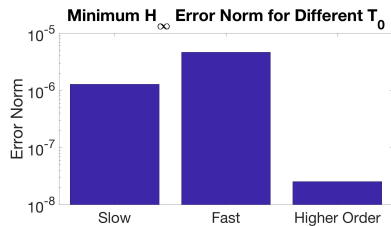


Fig. 7. The minimum H_∞ -norm of error for different T_0 transfer functions. Note that there is a logarithmic scale for the y-axis.

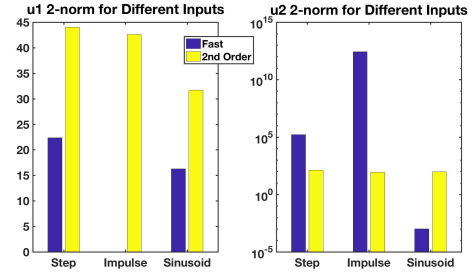


Fig. 8. The 2-norms of controller-generated signals u_1 and u_2 for a step input. These signals were generated for different T_0 transfer functions. Note that the plot on the right has a logarithmic scale for the y-axis.

IV. CONCLUSIONS

In this paper, we provide an initial proof of concept that optimal control techniques may be employed to create an improved controller for implementation in a prosthetic limb. Two separate controllers can be added into a prosthesis-user system in order to process user EMG data and prosthesis output, and produce an actuation signal for the prosthesis and feedback stimulation for the user. These controllers are tuned by minimizing the H_∞ -norm of the closed-loop system.

The current study assumes each component of the system to be linear to demonstrate the feasibility of such an approach. However, in a real-life setting, these components can be estimated from experimental data, and if nonlinear, can be approximated to be linear with model uncertainty absorbing the nonlinearities. That is, a set of systems can be specified where the nominal model is linear and the uncertainty in the set encompasses all systems that add nonlinearity to the nominal model; then robust controller synthesis can be employed for model matching in this framework. Future work includes derivation of realistic models for H derived from actual human data, P derived from physical laws, and a T_0 that approximates a healthy human system.

REFERENCES

- [1] E. Lumpkin and M. Caterina, "Mechanisms of sensory transduction in the skin," *Nature*, vol. 445, no. 7130, pp. 858–865, 2007.
- [2] V. E. Abraira and D. D. Ginty, "The sensory neurons of touch," *Neuron*, vol. 79, no. 4, pp. 618–639, 2013.
- [3] D. Farina, I. Vujaklija, M. Sartori, T. Kapelner, F. Negro, N. Jiang, K. Bergmeister, A. Andalib, J. Principe, and O. C. Aszmann, "Man/machine interface based on the discharge timings of spinal motor neurons after targeted muscle reinnervation," *Nat. Biomed. Eng.*, vol. 1, p. 0025, 2017.
- [4] J. Betthauser, C. Hunt, L. Osborn, M. Masters, G. Lévy, R. Kaliki, and N. Thakor, "Limb position tolerant pattern recognition for myoelectric prosthesis control with adaptive sparse representations from extreme learning," *IEEE Trans. Biomed. Eng.*, 2017. doi: 10.1109/TBME.2017.2719400
- [5] L. Osborn, H. Nguyen, J. Betthauser, R. Kaliki, and N. Thakor, "Biologically inspired multi-layered synthetic skin for tactile feedback in prosthetic limbs," in *Conf. IEEE Eng. Med. Biol.*, 2016, pp. 4622–4625.
- [6] B. Tee, A. Chortos, A. Berndt, A. K. Nguyen, A. Tom, A. McGuire, Z. C. Lin, K. Tien, W.-G. Bae, H. Wang, P. Mei, H.-H. Chou, B. Cui, K. Deisseroth, T. N. Ng, and Z. Bao, "A skin-inspired organic digital mechanoreceptor," *Science*, vol. 350, no. 6258, pp. 313–316, 2015.
- [7] M. Schiefer, D. Tan, S. Sidek, and D. Tyler, "Sensory feedback by peripheral nerve stimulation improves task performance in individuals with upper limb loss using a myoelectric prosthesis," *J. Neural Eng.*, vol. 13, no. 1, pp. 016001, 2015.

- [8] L. Osborn, M. Fifer, C. Moran, J. Betthausen, R. Armiger, R. Kaliki, and N. Thakor, "Targeted transcutaneous electrical nerve stimulation for phantom limb sensory feedback," in *Conf. IEEE Biomed. Circuits Syst.*, 2017, pp. 1–4.
- [9] C. Oddo, S. Raspopovic, F. Artoni, A. Mazzoni, G. Spigler, F. Petrini, F. Giambattistelli, F. Vecchio, F. Miraglia, L. Zollo, G. Pino, D. Camboni, M. Carrozza, E. Guglielmelli, P. Rossini, U. Faraguna, and S. Micera, "Intraneural stimulation elicits discrimination of textural features by artificial fingertip in intact and amputee humans," *eLife*, vol. 5, pp. e09148, 2016.
- [10] L. Osborn, H. Nguyen, R. Kaliki, and N. Thakor, "Prosthesis grip force modulation using neuromorphic tactile sensing," in *Myoelec. Controls Symp.*, 2017, pp. 188–191.
- [11] Y. Cho, K. Liang, F. Folowosele, B. Miller, and N. Thakor, "Wireless Temperature Sensing Cosmesis for Prosthetics," in *Conf. IEEE Rehabil. Robot.*, 2007, pp. 672–677.
- [12] A. Polishchuk, W. Navaraj, H. Heidari, and R. Dahiya, "Multisensory Smart Glove for Tactile Feedback in Prosthetic Hand," in *Procedia Eng.*, vol. 168, pp. 1605–1608, 2016.
- [13] M. Jimenez, and J. Fishel, "Evaluation of Force, Vibration and Thermal Tactile Feedback in Prosthetic Limbs," in *IEEE Haptics Symp.*, 2014, pp. 437–441.
- [14] E. Engeberg and S. Meek, "Adaptive Sliding Mode Control for Prosthetic Hands to Simultaneously Prevent Slip and Minimize Deformation of Grasped Objects," in *IEEE ASME Trans. Mechatron.*, vol. 18, no. 1, pp. 376–385, Feb. 2013.
- [15] L. Osborn, R. Kaliki, A. Soares, and N. Thakor, "Neuromimetic event-based detection for closed-loop tactile feedback control of upper limb prostheses," *IEEE Trans. Haptics*, vol. 9, no. 2, pp. 196–206, 2016.
- [16] M. Shanechi, "Brain-Machine Interface Control Algorithms," *IEEE Trans. Neural Syst. Rehabil. Eng.*, vol. 25, no. 10, pp. 1725–1734, Oct. 2017.
- [17] M. Tsai, and D. Gu, "Robust and Optimal Control: a Two-Port Framework Approach," Springer, 2014.
- [18] M. De Gregorio, V. Santos, "Precision grip responses to unexpected rotational perturbations scale with axis of rotation," *J. Biomech.*, vol. 46, pp. 1098–1103, 2013.
- [19] D. C. Youla, H. A. Jabri, J. J. Bongiorno: Modern Wiener-Hopf design of optimal controllers: part II, *IEEE Trans. Automat. Contr.*, AC-21 (1976) pp319?338
- [20] L. Zollo, S. Roccoella, E. Guglielmelli, M. Carrozza, P. Dario, "Biomechatronic design and control of an anthropomorphic artificial hand for prosthetic and robotic applications," *IEEE ASME Trans. Mechatron.*, vol. 12, no. 4, pp. 418–429, 2007.